Journal of Statistical Mechanics:
Theory and Experiment

PAPER: BIOLOGICAL MODELLING AND INFORMATION

Discontinuous percolation transitions in growing networks

Journal of Statistical Mechanics: Theory and Experiment
An IOP and SISSA journal

PAPER: Biological modelling and information

Discontinuous percolation transitions in growing networks

S M Oh[1], S-W Son[2,3] and B Kahng[1]

[1] CCSS, CTP and Department of Physics and Astronomy, Seoul National University, Seoul 08826, Republic of Korea
[2] Department of Applied Physics, Hanyang University, Ansan 15588, Republic of Korea
[3] Asia Pacific Center for Theoretical Physics, Pohang 37673, Republic of Korea
E-mail: dotoa@snu.ac.kr, sonswoo@hanyang.ac.kr and bkahng@snu.ac.kr

Received 4 May 2019
Accepted for publication 3 June 2019
Published 19 August 2019

Online at stacks.iop.org/JSTAT/2019/083502
https://doi.org/10.1088/1742-5468/ab3110

Abstract. Growing networks are ubiquitous in the real world, ranging from co-authorship socio-networks to protein interaction bio-networks. It is conventionally known that the giant cluster in such growing networks emerges continuously with infinite-order critical behavior. In this study, we show that when the growth of large clusters is suppressed with global information, the continuous percolation transition changes to a discontinuous transition with an abrupt jump of the order parameter at a delayed transition point p_c. Moreover, a second-order-type critical behavior appears in a wide region of the link occupation probability before the system explodes, in which while the largest cluster has not grown to the extensive size of the system yet, the mean cluster size diverges. Far below p_c, the property of the infinite-order transition still remains. Accordingly, the features of infinite-order, second-order, and first-order transitions all occur in a single framework when the infinite-order transition is suppressed. We present a simple argument to explain the underlying mechanism of these abnormal transition behaviors. Finally, we show that this result is universal by examining percolation transitions of a protein-interacting-network model.

Keywords: cluster aggregation, percolation problems, phase diagrams, protein interaction networks

1742-5468/19/083502+22$33.00

Contents

1. Introduction 2

2. Model: r-GRN model 4

3. Cluster size distribution $n_s(p)$ 6

4. Two transition points, p_b and p_c 8
4.1. For finite S_R 10
4.2. For infinite S_R 11

5. τ (p) in the critical region and total number of clusters 12

6. Universal behavior 14

7. Discussion 16

8. Summary 19
Acknowledgment 20
Appendix. Rate equations of the r-GRN model 20

References 21

1. Introduction

Growing networks are ubiquitous in the real world. Co-authorship networks [1, 2], the World Wide Web (WWW) [3], and protein interaction networks [4–6] are good examples. In growing networks, system size, i.e. the number of nodes, grows as time goes, such as a co-authorship network [1, 2] grows as a new graduate student writes the first paper with other colleagues, the WWW grows as a new website opens, and the protein interaction network grows by a gene mutation. Callaway *et al* [7] introduced a growing random network (GRN) model, where a node, representing a person, a web page, or a protein, is present in the system at the beginning. At each time step, a new node is added, then a pair of unconnected nodes, which is chosen randomly among all existing nodes, forms a link with probability p. The connected clusters represent social communities, groups of hyperlinked websites, or protein complexes binding together. As p increases, a percolation transition (PT) occurs at a certain transition point p_c, beyond which a macroscopic-scale large cluster emerges. The PT of the GRN model follows an infinite-order Berezinskii–Kosterlitz–Thouless (BKT) transition [7–14].

Berezinskii, Kosterlitz and Thouless discovered an infinite-order topological phase transition in the early 1970s. Since then, its notion has been widely used for understanding diverse phenomena ranging from the superfluid-normal phase transition [13] and quantum phase transitions [14] in physical systems to PTs of growing networks [7, 15] in interdisciplinary areas. Following the basic idea of Paul Ehrenfest's in 1933 [16], phase transitions are normally classified by the lowest derivative of the free energy that

J. Stat. Mech. (2019) 083502

is discontinuous at a transition point. First-order phase transitions exhibit a discontinuity in the order parameter and finite fluctuations, and second-order phase transitions are continuous in the first derivative of the free energy, but diverges in the second derivative such as the susceptibility at a transition point. The latter transition also has features that the correlation length diverges and the correlation function decays in a power-law manner at the transition point. Under this classification scheme, there could in principle be higher-order phase transitions.

In the GRNs, the order parameter, i.e. the relative giant cluster size, $G(p)$ is zero for $p < p_c$ and increases continuously for $p > p_c$ in the essentially singular form

$$G(p) \sim \exp(-a/\sqrt{p - p_c}), \tag{1}$$

where a is a positive constant. Thus, the PT is infinite-order. In this case, the cluster size distribution $n_s(p)$ follows a power law $n_s \sim s^{-\tau}$ without any exponential cutoff in the entire region of $p < p_c$ [6, 7, 15, 17]. Thus, the region $p < p_c$ is often referred to as the critical region. The exponent τ decreases with increasing p and approaches $\tau = 3$ as $p \to p_c$ from below [6, 15]. Thus, the mean cluster size, $\langle s \rangle \equiv \sum_s s^2 n_s$, is finite for $p \leqslant p_c$. Moreover, for $p > p_c$, $n_s(p)$ of finite clusters decays exponentially. Thus, $\langle s \rangle$ is finite. These properties of a PT of growing networks are different from those of a second-order PT of static networks [7, 17–21].

The type of a phase transition can change by long-range interactions. For instance, a PT in one dimension is changed to an infinite-order transition by $1/r^2$ long-range connections [22]. Similarly, a PT can be changed by global suppression effects [23]. A second-order PT in two dimensions can be changed to a first-order one when formation of a spanning cluster is suppressed [24]. We remark that such PT-type changes due to long-range connections or global suppression effects have been investigated only in the static networks, where the system size is fixed; however, it has rarely investigated in growing networks.

Suppression dynamics may arise in growing networks. For instance, the co-authorship network [2] grows as a new graduate student joins a group and writes a paper together with group members. As a research group becomes larger, the group can become less efficient functionally in some aspects; thus, new students are less likely to join such a group and thus the growth of large groups can be suppressed. As new students join small or medium groups, those groups grow in size. Those large clusters can merge as postgraduates transfer to another large group, leading to an abrupt size increase of the largest cluster as we observed in the real-world data [2]. The evolution of such a co-authorship network does not proceed by purely random connections, but there exists some suppression mechanism against the growth of large clusters. Moreover, the suppression effect can also arise in the WWW by the reasons of inaccessibility and invisibility.

Here, we investigate how the infinite-order PT of growing networks is changed by the suppression effect. In fact, the current authors considered such a problem recently and showed that indeed the transition type changes from infinite-order to discontinuous transition. The critical behavior in the subcritical region $p < p_c$, i.e. the power-law decay behavior of the cluster size distribution has different feature: infinite-order-type and second-order-type properties [25]. However, properties of the phase transition were considered in some specific cases and derivations were not reported in detail. Here, we

J. Stat. Mech. (2019) 083502

investigate the cluster size distribution and critical behaviors as a parameter of suppression strength is varied. Moreover, we consider if such properties emerge in another growing model, finding that such properties appear as universal features.

To implement this, we modify the GRN model by including the suppression mechanism as follows: At each time step, a node is added to the system. To add a link, we select two nodes—a node from a portion of the smallest clusters and the other node from among all the nodes. They are connected with probability p. Because a node belonging to small clusters has twice the chance to be linked, while a node in large clusters has a single chance, the growth of large clusters is practically suppressed. The dynamic rule becomes global in the process of sorting out the portion of the smallest clusters among all cluster sizes. This model is called the restricted growing random network (r-GRN) model [25] following the restricted Erdős–Rényi (r-ER) model [26–29], which is static.

This paper is organized as follows: in section 2, we introduce a dynamic rule of the r-GRN model. In section 3, the cluster size distribution is derived explicitly, and its implication is discussed. In section 4, the two critical points are determined using the generating function technique. In section 5, the exponent $\tau(p)$ of the cluster size distribution is determined explicitly as a function of p in a limited case. We also obtain the total number of clusters per node. In section 6, we find a similar result in a different restricted growing network model based on the protein interaction network (PIN) model and argue that the obtained results are universal. In section 7, we discuss the implications of our results. In section 8, we summarize the results of this paper. In the appendix, we recall the rate equation of the cluster size distribution as a function of link density p and time t, previously obtained.

2. Model: r-GRN model

The r-GRN model starts with a single node. At each time step, a new node is added to the system. Thus, the total number of nodes at time step t becomes $N(t) = t + 1$. As time goes on, clusters of connected nodes form. At each time step, we classify clusters into two sets, set $\mathbf{R}$ and its complement set $\mathbf{R^c}$, according to their sizes. Set $\mathbf{R}$ contains $\lceil gN(t) \rceil$ nodes belonging to the smallest clusters, whereas set $\mathbf{R^c}$ contains the nodes belonging to the rest large clusters. $g \in [0, 1]$ is a parameter that controls the size of $\mathbf{R}$. Let c_i denote the ith cluster in ascending order of cluster size. Suppose that the $(k-1)$th cluster satisfies the condition $\sum_{i=1}^{k-1} s(c_i) < \lceil gN \rceil \leqslant \sum_{i=1}^{k} s(c_i)$, where $s(c_i)$ denotes the size of the cluster with index c_i. Then, set $\mathbf{R}(t)$ contains all the nodes belonging to the $k-1$ smallest clusters and $\lceil gN \rceil - \sum_{i=1}^{k-1} s(c_i)$ nodes randomly selected from the kth smallest cluster. The complement set $\mathbf{R^c}$ contains the remaining (largest) clusters. Next, one node is randomly selected from set $\mathbf{R}(t)$ and another is selected from among all the nodes. A node in the set of smaller clusters has twice the chance of being linked, while a node in the set of larger clusters has one chance. Then, a link is added between the two selected nodes with link occupation probability p. The selection rule becomes global in the process of sorting out the portion of the smallest clusters among all clusters. Moreover, it suppresses the growth of large clusters by allowing less chance to be linked. This link connection process is visualized in figure 1 for the restricted fraction

J. Stat. Mech. (2019) 083502

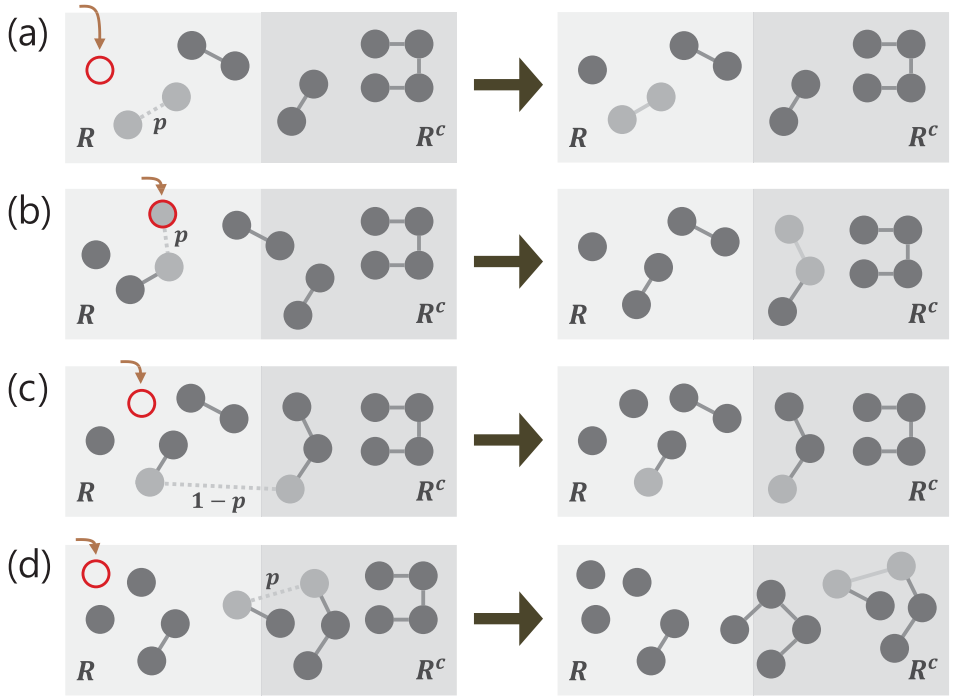

Figure 1. Schematic illustration of the r-GRN model with $g = 0.4$. Nodes are represented by the circles. $\mathbf{R}(t)$ is represented by the light gray region and $\mathbf{R^c}(t)$ is done by the dark grey region. The solid line between two nodes represents a link. In (a), the system starts at five clusters with sizes $(1, 1, 2, 2, 4)$, respectively, and the total number of nodes $N(t) = 10$ with $S_R = 2$ and $\lceil gN \rceil = 4$ at time $t = 9$. After one time step, a new node (red open circle) is added to the system. Then the total number of nodes $N(t)$ becomes 11 with $S_R = 2$ and $\lceil gN \rceil = 5$ at $t = 10$. Two isolated nodes (filled light grey) are selected from $\mathbf{R}$ and are merged and become one cluster of size two. But S_R remains two. (b) At the next step, a new node is added to the system, and so $N(t) = 12$, $S_R = 2$, and $\lceil gN \rceil = 5$ at $t = 11$. In this case, just one node of the largest cluster of size two in set $\mathbf{R}$ moves to set $\mathbf{R^c}$. The newly added node is merged with the cluster of size two in $\mathbf{R}$, generating a cluster of size three. This cluster moves to set $\mathbf{R^c}$ and the cluster of size two on the boundary between $\mathbf{R}$ and $\mathbf{R^c}$ moves to $\mathbf{R}$. Set $\mathbf{R}$ contains three clusters and five nodes and $S_R = 2$. Set $\mathbf{R^c}$ contains two clusters and seven nodes. (c) At the next step, a new node is added to the system with $N(t) = 13$, $S_R = 2$, and $\lceil gN \rceil = 6$ at $t = 12$. Two nodes are selected, but they are not connected with probability $1 - p$. (d) At the next step, a new node is added with $N(t) = 14$, $S_R = 2$, and $\lceil gN \rceil = 6$ at $t = 13$. And just one node of the largest cluster of size two in set $\mathbf{R}$ moves to set $\mathbf{R^c}$ again as in (b). A cluster of size two in $\mathbf{R}$ and the cluster of size three in $\mathbf{R^c}$ are merged and generate a cluster of size five, and then this cluster belongs to $\mathbf{R^c}$. The cluster of size four in $\mathbf{R^c}$ lies on the boundary between $\mathbf{R}$ and $\mathbf{R^c}$. At the same time, the cluster of size two on the boundary moves to $\mathbf{R}$. S_R becomes four. Some nodes of the cluster of size S_R on the boundary are regarded as the elements of set $\mathbf{R}$.

J. Stat. Mech. (2019) 083502

$g = 0.4$ as an example. This restriction rule is initially introduced in [27] and modified in [28, 29].

We define the size of the largest cluster in set **R** as $S_R(p,t)$ for a given p at time t, which determines the size of the boundary cluster(s) between the two sets. It depends on the fraction g [28]. Thus, when $g = 1$, which means that S_R is equal to the size of the giant cluster, denoted as $GN(t)$, this model reduces to the original GRN model [7]. It has been found previously that the GRN model exhibits a continuous infinite-order phase transition at $p_c = 1/8$ [7]. However, when $g \to 0$, $S_R = 1$, and an isolated node in **R**, is merged with a node in $\mathbf{R^c}$ with link occupation probability p.

3. Cluster size distribution $n_s(p)$

Let us define the cluster number density $n_s(p,t)$ for a given p at time step t as the number of clusters of size s divided by the current number of nodes $N(t)$ at t. In our previous studies [25], we derived the rate equations according to the cluster size s comparing to S_R for the cluster size distribution $N(t)n_s$. For convenient readability, those rate equations are rewritten in the appendix.

Here we solve the rate equation of $n_s(p)$ for a given g. First, when $s = 1$, the rate equation becomes $n_1 = -p(1 + \frac{1}{g})n_1 + 1$ for $S_R > 1$ and $n_1 = -p(n_1 + 1) + 1$ for $S_R = 1$. Thus, $n_1(p)$ becomes

$$n_1 = \begin{cases} \frac{1}{1+p(1+\frac{1}{g})} & S_R(p) > 1 \quad (p > p_1), \\ \frac{1-p}{1+p} & S_R(p) = 1 \quad (p < p_1). \end{cases} \tag{2}$$

The two solutions become the same at $p = (1-g)/(1+g)$, as shown in figure 2(e). This p is denoted as p_1. For $g = 0.4$, $p_1 = 0.428\,5714\ldots$.

Next, when $s = 2$, the rate equations are as follows: $n_2 = p[(n_1 n_1/g) - 2n_2(1 + 1/g)]$ for $S_R > 2$; $n_2 = p[(n_1 n_1/g) - 2n_2 - (1 - n_1/g)]$ for $S_R = 2$; $n_2 = p(n_1 - 2n_2)$ for $S_R = 1$. We obtain n_2 as follows:

$$n_2 = \begin{cases} \frac{p\frac{{n_1}^2}{g}}{1+2p(1+\frac{1}{g})} & S_R > 2 \quad (p > p_2), \\ \frac{p[\frac{{n_1}^2}{g} - (1-\frac{n_1}{g})]}{1+2p} & S_R = 2 \quad (p_1 < p < p_2), \\ \frac{pn_1}{1+2p} & S_R = 1 \quad (p < p_1). \end{cases} \tag{3}$$

Two kinks (crossovers) exist in $n_2(p)$, as shown in figure 2(f). The position p of the first kink is just p_1, and that of the second kink is determined by setting n_2 for $S_R > 2$ equal to that for $S_R = 2$. This position is denoted as p_2. For $g = 0.4$, $p_2 = 0.565\,3082\ldots$.

In general, when $s > 1$, the cluster size distribution $n_s(p)$ can be obtained from the rate equations in the steady state as follows:

https://doi.org/10.1088/1742-5468/ab3110

J. Stat. Mech. (2019) 083502

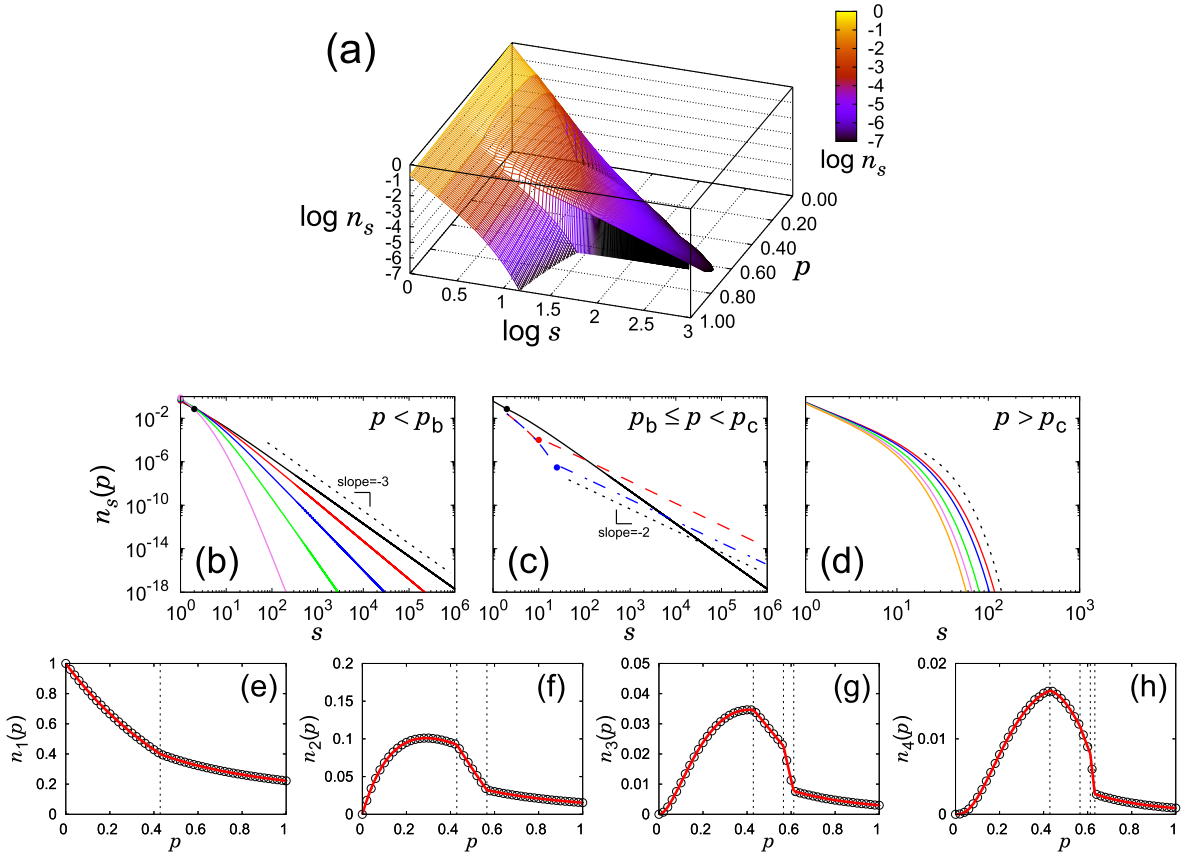

Figure 2. Cluster size distribution $n_s(p)$ as a function of s and p for given g: In this case, $g = 0.4$ are taken. (a) Three-dimensional plot of $n_s(p)$ as a function of s and p. A clear discontinuous pattern exists. Plots (b)–(d) are obtained with several fixed p for $n_s(p)$. (b) For $p < p_b$, $n_s(p)$ asymptotically follows the power law $\sim s^{-\tau}$ with $\tau > 3$. The slope of the dotted guide line is -3. Solid lines are obtained for $p = 0.472\,576 \approx p_b$, 0.4, 0.3, 0.2, and 0.1 from right to left. (c) For $p_b \leqslant p < p_c$, in the small-cluster-size region, $n_s(p)$ decays exponentially up to S_R and then exhibits power-law decay behavior with $2 < \tau \leqslant 3$. Solid, dashed, and dashed-dotted lines represent for p_{S_R} with $S_R = 2$, 10 and 25, respectively. Dotted line is a guide line with slope of -2. (d) For $p \geqslant p_c$, $n_s(p)$ for finite clusters shows exponentially decay distributions. Solid curves represent $n_s(p)$ for $p = 0.6596$, 0.7, 0.8, 0.9, and 1.0 from right to left. The dotted curve is an exponentially decaying guide curve. Plots (e)–(h) are obtained with several values of s for $n_s(p)$. (e) The plot of $n_1(p)$ versus p. A crossover exists at p_1. (f) The plot of $n_2(p)$ versus p. Two crossover behaviors occur at p_1 and p_2, where $p_1 < p_2$. (g) and (h) Plots of $n_3(p)$ and $n_4(p)$ versus p, respectively. Symbols represent simulation results, and solid lines are analytical results. Dotted vertical lines represent p_{S_R} for $S_R = 1$, 2, 3 and 4 at $p_{S_R=1} = 0.428\,5714$, $p_{S_R=2} = 0.565\,3082$, $p_{S_R=3} = 0.612\,0164$, and $p_{S_R=4} = 0.632\,7279$, which are close to the simulation results.

J. Stat. Mech. (2019) 083502

$$n_s(p) = \begin{cases} \dfrac{p\sum_{i,j=1}^{\infty} \frac{in_i jn_j}{g}\delta_{i+j,s}+\delta_{1s}}{1+sp(1+\frac{1}{g})} & s < S_R, \\ \dfrac{p\left[\sum_{i,j=1}^{\infty} \frac{in_i jn_j}{g}\delta_{i+j,s}-\left(1-\sum_{k=1}^{S_R-1}\frac{kn_k}{g}\right)\right]}{1+sp} & s = S_R, \\ \dfrac{p\left[\sum_{j=1}^{\infty}\sum_{i=1}^{S_R-1} \frac{in_i jn_j}{g}\delta_{i+j,s}+\sum_{j=1}^{\infty}\delta_{S_R+j,s}jn_j\left(1-\sum_{k=1}^{S_R-1}\frac{kn_k}{g}\right)\right]}{1+sp} & s > S_R. \end{cases} \quad (4)$$

There exist s kinks on the curve n_s at $p_1, \cdots, p_s$ in ascending order of p. The position of the last kink p_s is determined by setting n_s for $S_R > s$ equal to n_s for $S_R = s$. For convenience, we use the index as S_R to avoid confusion with the index of cluster size s. The positions p_{S_R} as a function S_R are listed in table 1. As shown in figures 2(e)–(h), the interval between two successive crossover points becomes narrower with increasing S_R. The position p_{S_R} seems to converge to a certain value, p_∞, in a power-law form of $p_\infty - p_{S_R}$ as a function of S_R asymptotically as shown in figure 3. Here p_∞ is estimated to be 0.659 48(1). Figures 2(b)–(d) show the distributions n_s versus s for a given fixed p, which corresponds to the $(\log n_s, \log s)$ plane of the three-dimensional plot of $n_s(p)$ in figure 2(a).

4. Two transition points, p_b and p_c

From the cluster size distribution $n_s(p)$ for given p, we find that there exist two transition points, say p_b and p_c, which characterize the following three distinct intervals on the line of p: (i) For $p < p_b$, $n_s(p)$ follows the power law $n_s(p) \sim s^{-\tau}$ for $s > S_R$ with exponent $\tau > 3$, whereas it decays exponentially as a function of s for $s < S_R$. (ii) For $p_b \leqslant p < p_c$, $n_s(p)$ also follows a power law with exponent τ for $s > S_R$. Particularly, the exponent τ decreases continuously from $\tau = 3$ to 2 as p is increased from p_b to p_c. For $s < S_R$, $n_s(p)$ decays exponentially as a function of s. (iii) For $p > p_c$, a giant cluster is generated and the distribution of the remaining finite clusters decays exponentially as a function of s.

The power-law behavior of $n_s(p)$ with $\tau > 3$ in the region (i) is inherited from the infinite-order transition of the GRN model [7]. Thus the region (i) is regarded as an infinite-order-type critical region. Meanwhile, in the region (ii), because $2 < \tau < 3$, the mean cluster size diverges. Thus the region (ii) is regarded as a second-order-type critical region. It is worth noting that while the critical behavior occurs at a critical point in a prototypical second-order transition, here it occurs in the entire region (ii). At p_c^-, $\tau = 2$. This means that clusters are extremely heterogeneous and further suppression of the largest cluster leads to a discontinuous transition. This feature will be discussed later in section 7. Indeed, a discontinuous transition occurs at p_c. Both transition points for different g values are listed in table 2.

To determine p_b and p_c, here we introduce the generating function $f(x)$ of the probability sn_s that a randomly chosen node belongs to the cluster of size s, defined as

J. Stat. Mech. (2019) 083502

Table 1. Values of p_{S_R} as a function of S_R for $g = 0.4$.

S_R	p_{S_R}
1	0.428 571 4285(1)
2	0.565 308 2407(1)
3	0.612 016 4684(1)
4	0.632 727 9058(1)
5	0.643 336 2667(1)
6	0.649 281 4220(1)
7	0.652 822 6406(1)
8	0.655 026 2003(1)
9	0.656 442 9142(1)
10	0.657 376 9871(1)
11	0.658 005 2394(1)
12	0.658 434 6536(1)
13	0.658 732 0681(1)
14	0.658 940 3439(1)
15	0.659 087 5632(1)
16	0.659 192 4579(1)
17	0.659 267 7124(1)
18	0.659 322 0275(1)
19	0.659 361 4370(1)
20	0.659 390 1656(1)
∞	0.659 48(1)

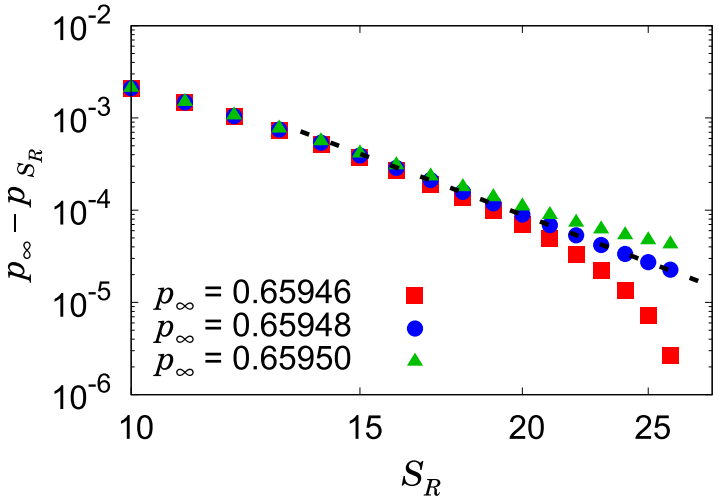

Figure 3. Plot of $p_\infty - p_{S_R}$ versus S_R for $g = 0.4$. When $p_\infty = 0.659\,48(1)$, a power-law decay appears.

$$f(x) \equiv \sum_{s=1}^{\infty} s n_s x^s, \tag{5}$$

where x is the fugacity in the interval $0 < x < 1$. The giant cluster size G is obtained as $G = 1 - \sum_{s=1}^{\infty} s n_s = 1 - f(1)$. The mean cluster size is obtained as $\langle s \rangle = \sum_{s=1}^{\infty} s^2 n_s = f'(1)$, where the prime represents the derivative with respect to x. To determine p_b (p_c), we consider the case of S_R being finite (infinite).

Table 2. Numerical estimates of the transition points p_b and p_c. The critical exponents τ are calculated at $p = p_b$ and p_c for $g = 0.1 - 0.9$. We note that the exponent τ at p_c becomes difficult to obtain as g approaches one.

g	p_b	p_c	ΔG	$\tau(p_b)$	$\tau(p_c)$
0.1	1/2	0.905(1)	0.900(1)	3.00(1)	2.00(1)
0.2	1/2	0.817(1)	0.800(1)	3.00(1)	2.00(1)
0.3	1/2	0.736(1)	0.700(1)	3.00(1)	2.00(1)
1/3	1/2	0.710(1)	0.666(1)	3.00(1)	2.00(1)
0.4	0.473(1)	0.660(1)	0.600(1)	3.00(1)	2.00(1)
0.5	0.440(1)	0.587(1)	0.500(1)	3.00(1)	2.00(1)
0.6	0.405(1)	0.516(1)	0.400(1)	3.00(1)	2.00(1)
0.7	0.367(1)	0.447(1)	0.300(1)	3.00(1)	1.99(1)
0.8	0.323(1)	0.376(1)	0.200(1)	3.00(1)	1.99(1)
0.9	0.268(1)	0.297(1)	0.100(1)	3.00(1)	1.8(2)
1.0	1/8	1/8	0	3	—

4.1. For finite S_R

When S_R is finite, we derive the recurrence relation for n_s. First, when $S_R = 1$, the rate equations in the steady state are simply reduced as follows:

$$n_1 = -p(n_1 + 1) + 1, \tag{6}$$

$$n_s = p\big[(s-1)n_{s-1} - sn_s\big] \quad \text{for} \quad s > 1. \tag{7}$$

Then, one can obtain the generating function $f(x)$ as

$$f(x) = -xpf'(x) - px + x + px^2 f'(x) + pxf(x). \tag{8}$$

The giant cluster size G is $G = 1 - \sum_{s=1}^{\infty} sn_s = 1 - f(1) = 0$. The mean cluster size is obtained as $\langle s\rangle = \sum_{s=1}^{\infty} s^2 n_s = f'(1) = 1/(1-2p)$. So the mean cluster size diverges at $p_b = 1/2$. If this value is larger than p_1 for a given g, then we move to $S_R = 2$. When $S_R = 2$, $G = 0$ and $\langle s\rangle = f'(1) = 1/[1 - 4p + (2pn_1/g)]$.

Generally, for finite S_R, we obtain the relation

$$\begin{aligned} f(x) + xpf'(x) = x + p\Big[&\sum_{s=1}^{S_R-1} sx^s\Big(-\frac{1}{g}sn_s\Big) - S_R x^{S_R}\Big(1 - \frac{1}{g}\sum_{s=1}^{S_R-1} sn_s\Big) \\ &+ \sum_{s=1}^{S_R-1} \frac{sn_s}{g} x^s\big(xf'(x) + sf(x)\big) \\ &+ x^{S_R}(xf'(x) + S_R f(x))\Big(1 - \frac{1}{g}\sum_{s=1}^{S_R-1} sn_s\Big)\Big]. \end{aligned} \tag{9}$$

When $x = 1$, equation (9) may be written as $f(1)J(p) = J(p)$ for the range $p_{S_R-1} \leqslant p < p_{S_R}$, where $J(p) \equiv 1 - p\big[\sum_{s=1}^{S_R-1} \frac{s^2 n_s}{g} + S_R\big(1 - \sum_{s=1}^{S_R-1} \frac{sn_s}{g}\big)\big]$. Now, let us denote p satisfying $J(p) = 0$ as p^*. We can calculate these values p^* as S_R increases using equation (4) in the steady state. But p^* is always larger than p_{S_R} so $J(p)$ cannot

J. Stat. Mech. (2019) 083502

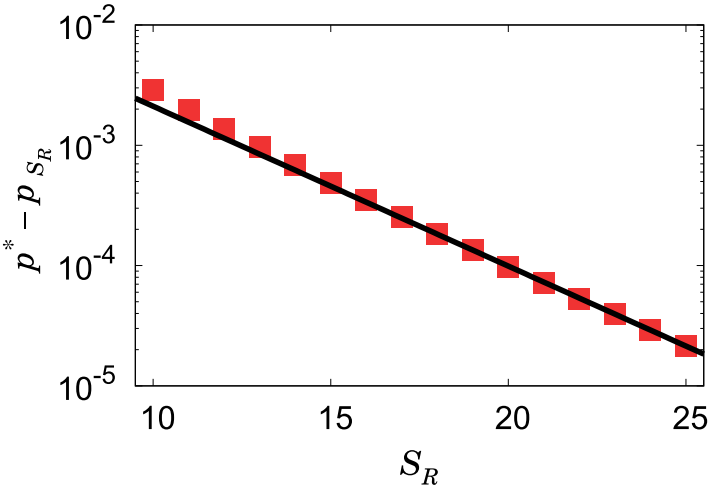

Figure 4. Semi-log plot of $p^* - p_{S_R}$ versus S_R. $p^* - p_{S_R}$ decays exponentially as S_R increases but it is always larger than zero for finite S_R values. So p^* is larger than p_{S_R} for any finite S_R.

be zero as shown in figure 4 for the case $g = 0.4$. Then we can obtain that $f(1) = 1$ for finite S_R and the relative giant cluster $G = 1 - f(1) = 0$.

At $x = 1$, plugging $f(1) = 1$ into the derivative of equation (9) with respect to x, we obtain that

$$f'(1) = \left[1 + 2p\left(\sum_{s=1}^{S_R-1} \frac{(S_R - s)sn_s}{g} - S_R\right)\right]^{-1} = \langle s \rangle. \tag{10}$$

To obtain p_b, once we set $S_R = 1$ and check whether a certain value of p less than p_{S_R} exists, say p_*, such that $\langle s \rangle^{-1} = 0$. If the solution exists, p_* is a critical point p_b and S_R is the size of the largest cluster in set $\mathbf{R}$. Otherwise, we increase S_R by one, and try to find a solution satisfying $\langle s \rangle^{-1} = 0$. We repeat these steps until the solution is found. The obtained values p_b for different g are listed in table 2. The existence of p_b below p_c implies that even though the order parameter $G(p)$ is zero for $p < p_c$, the mean cluster size $\langle s \rangle$ can diverge at p_b before p_c.

4.2. For infinite S_R

We consider the limit $S_R(p) = \infty$, which corresponds to the case $p > p_\infty$. In this case, equation (A.4) is valid for all cluster sizes s. Equations (A.4)–(A.6) reduce to the following two equations:

$$n_1 = \frac{1}{1 + (1 + \frac{1}{g})p}, \tag{11}$$

$$n_s = \frac{p}{1 + (1 + \frac{1}{g})sp} \sum_{j=1}^{s-1} \frac{j(s-j)n_j n_{s-j}}{g}, \tag{12}$$

J. Stat. Mech. (2019) 083502

where s is limited to finite clusters. The generating function associated with sn_s satisfies the following relation:

$$f(x) = -x(1+\frac{1}{g})\,pf'(x) + \frac{2}{g}pxf(x)\,f'(x) + x, \tag{13}$$

and in another form,

$$f'(x) = \frac{1-\frac{f(x)}{x}}{(1+\frac{1}{g})-\frac{2}{g}f(x)}\frac{1}{p}. \tag{14}$$

Performing numerical integration, we obtain $f(1)$ and $f'(1)$, which correspond to the order parameter $G(p)$ and $\langle s\rangle$ for given p and g in the region $p \geqslant p_\infty$. At p_∞, this order parameter value $G(p_\infty)$ is not zero but finite, indicating that the transition at p_∞ is first-order. Moreover, $G(p_\infty)$ represents the jump size of the order parameter ΔG of the discontinuous transition. We obtain the cluster size distribution using the equation (4), which follows a power law with $\tau \simeq 2$. Therefore, we think that $p_\infty = p_c$. The results for G and $1/\langle s\rangle$ in the entire region p are shown in figure 5 for $g = 0.2$, 0.4, and 0.6. Numerical data of p_b, p_c, ΔG, $\tau(p_b)$, and $\tau(p_c)$ for different g are listed in table 2. Indeed, the order parameters are discontinuous at p_c for different $g < 1$. We draw a phase diagram shown in figure 6 in the plane of (p, g).

5. $\tau(p)$ in the critical region and total number of clusters

When $p < p_c$, the cluster size distribution exhibits a critical behavior, it decays in a power law manner with exponent τ. This exponent τ depends on the link occupation probability p. This property is reminiscent of the feature of the BKT transition in thermal systems. However, the origin of the BKT transition in growing networks differs from that in thermal systems. To illustrate the origin of the critical behavior in growing networks, we consider a limit case with $g \to 0$ and $S_R = 1$. In this case, cluster merging dynamics occur only between isolated nodes and another cluster of any size. From equation (4), one can obtain the explicit form of $n_s(p)$ as follows:

$$n_s(p) = \frac{(s-1)!p^{s-1}n_1(p)}{(1+sp)(1+(s-1)\,p)\cdots(1+2p)}, \tag{15}$$

where $n_1(p)$ is $(1-p)/(1+p)$, and $S_R = 1$. Using the Stirling formula, the gamma function $\Gamma(z) = (z-1)!$ is rewritten as

$$\Gamma(z) \sim z^{z-\frac{1}{2}}\mathrm{e}^{-z}\sqrt{2\pi}\left(1+\frac{1}{12z}+\frac{1}{288z^2}-\frac{139}{51\,840z^3}-\frac{571}{2488\,320z^4}\right) \text{ as } |z|\to\infty,$$

one can obtain the asymptotic behavior of equation (15) as $n_s(p) = \frac{\Gamma(s)\Gamma(\frac{1}{p}+2)}{\Gamma(s+\frac{1}{p}+1)}n_1(p) \sim s^{-(1+\frac{1}{p})}$, where the critical exponent $\tau = 1+\frac{1}{p}$. Figure 7 shows τ as a function of p. Because the merging dynamics starts from $S_R = 1$, $\tau = 1+1/p$ appears in the envelope of $\tau(p)$. Thus, the addition of a new node into the system at each time step is a key factor that generates the critical region below the transition point p_c.

J. Stat. Mech. (2019) 083502

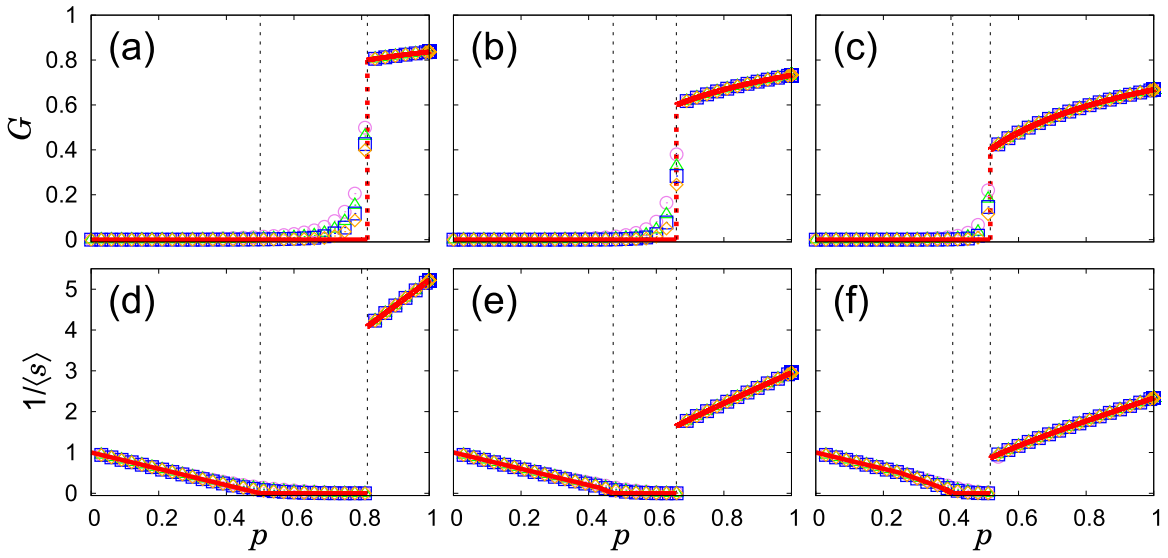

Figure 5. Plot of G and $1/\langle s\rangle$ as a function of p. For $g = 0.2$ in (a) and (d), $g = 0.4$ in (b) and (e), and $g = 0.6$ in (c) and (f), respectively. Symbols represent the simulation results for $N = 10^4$ (◯), 10^5 (△), 10^6 (□), and 10^7 (◇). Each data point was averaged over 10^3 times. The solid (red) lines are calculated from $f(1)$ and $f'(1)$ for G and $\langle s\rangle$, respectively. The two vertical dotted lines represent p_b and p_c ($p_b < p_c$).

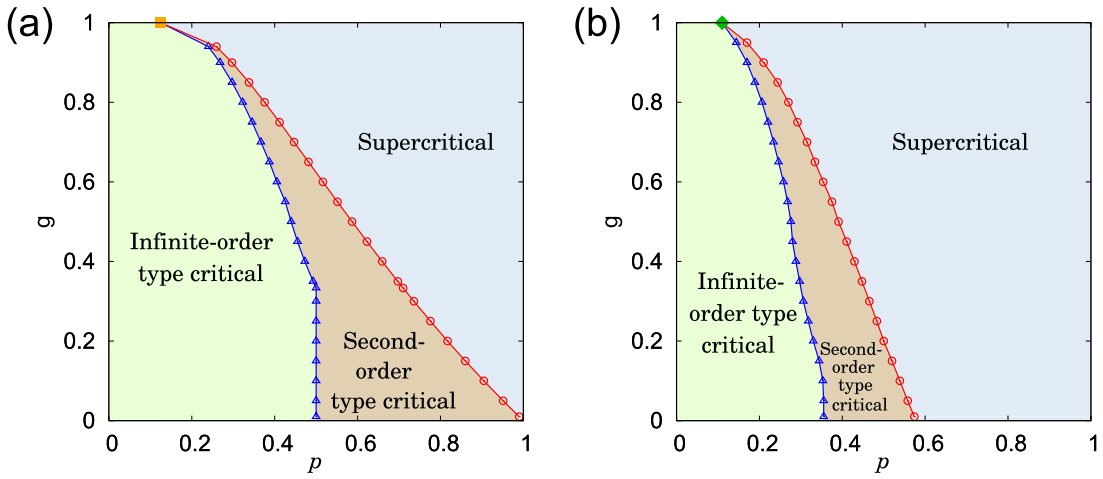

Figure 6. (a) and (b) show the phase diagrams of the r-GRN model and the r-PIN model with $\delta = 0.7$, respectively. Symbols △ and ◯ represent p_b and p_c. $n_s(p)$ decays following a power law with $\tau > 3$ in the infinite-order-type critical region and $2 < \tau < 3$ in the second-order-type critical region. Thus, the mean cluster size is finite and diverges, respectively. As g approaches one, the two phase boundaries converge to the conventional transition point $p_c = 1/8$ of the GRN model, represented by ■, and $p_c = 0.11(1)$ in the PIN model with $\delta = 0.7$, represented by ♦.

J. Stat. Mech. (2019) 083502

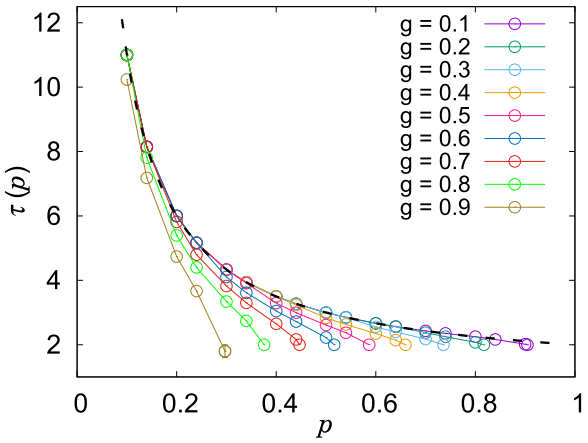

Figure 7. Plot of τ versus p for different g. τ becomes two as p approaches p_c for any g. The black dashed curve is a guide curve representing $1 + 1/p$, which is obtained from the limiting case $S_R = 1$, i.e. $g \to 0$.

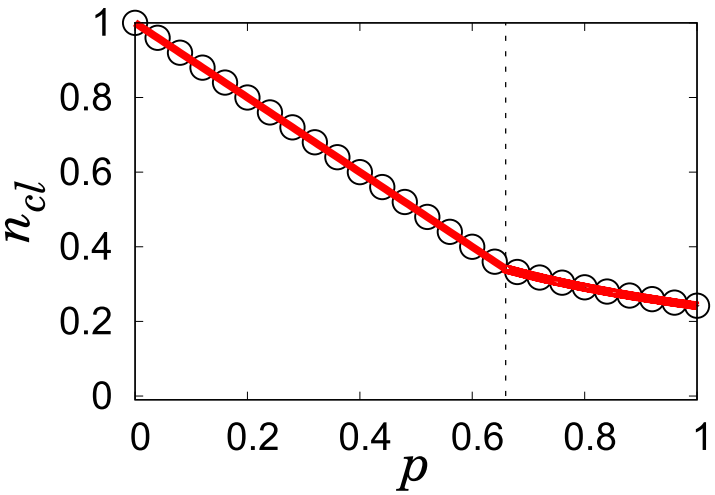

Figure 8. Plot of the total number of clusters n_{cl} versus p for $g = 0.4$. The red solid line is obtained from the rate equation integrating the cluster size distribution. The open circles represent the numerical simulation data for $N = 10^6$, averaged over 10^4 configurations. The black vertical dotted line represents p_c for $g = 0.4$.

The total number of clusters per site, $n_{cl}(p) \equiv \sum_{s=1}^{\infty} n_s(p)$, can be calculated from the rate equations by summing up $n_s(p)$ over all finite clusters in equation (4). Figure 8 shows $n_s(p)$ for $g = 0.4$. The circle symbols represent $n_s(p)$ obtained from numerical simulations. They are in agreement with theoretical results (solid line) for $g = 0.4$ in the entire p region.

6. Universal behavior

Protein interaction network (PIN) models are growing networks and also exhibit the BKT transitions [6]. Nodes in this network represent proteins and links connect functionally related proteins. Connected proteins form a proteome or protein complexes.

J. Stat. Mech. (2019) 083502

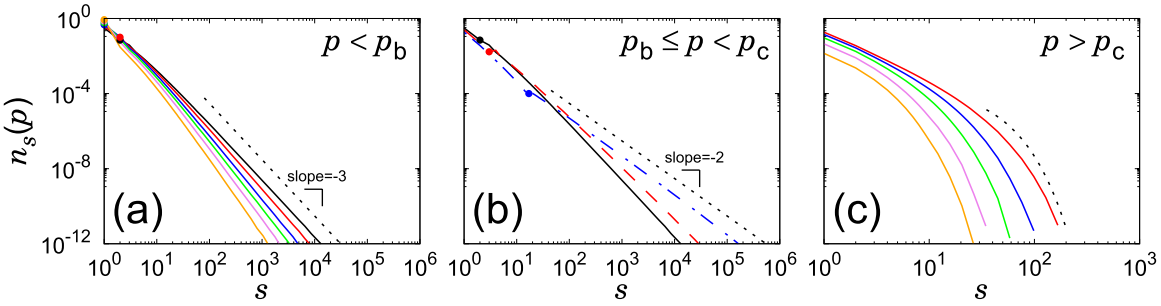

Figure 9. Plots of the cluster size distribution $n_s(p)$ of the r-PIN model as a function of s in different p regions. We binned simulation data logarithmically for $N = 2^{14} \times 10^4$ averaged over 10^3 configurations. $g = 0.4$ and $\delta = 0.7$ are taken. Three cases of $n_s(p)$ are distinguished: (a) For $p < p_b$, $n_s(p)$ asymptotically follows the power law $\sim s^{-\tau}$ with $\tau > 3$. The slope of the dotted guide line is -3. Solid lines are obtained for $p = 0.29 \approx p_b$, 0.25, 0.20, 0.15, 0.10, and 0.05 from right to left. (b) For $p_b \leqslant p < p_c$, in the small-cluster-size region, $n_s(p)$ decays exponentially and then exhibits power-law decay behavior with $2 < \tau \leqslant 3$. Solid (black), dashed (red), and dashed-dotted (blue) lines represent p_{S_R}, where $S_R = 2(p = 0.29)$,$3(p = 0.35)$, and 17 ($p = 0.423$), respectively. Two dotted lines are guidelines with slopes of -2 and -3. (c) For $p \geqslant p_c$, $n_s(p)$ for finite clusters shows exponentially decaying distributions. Solid curves represent $p = 0.43$, 0.50, 0.60, 0.75, and 0.90 from right to left. The dotted curve is an exponentially decaying guide curve.

The proteome network is a usually sparse graph with a small mean degree. Inspired from the biological process, several minimal models for the evolution of PIN were introduced [30]. Here we recall the PIN model proposed in [4, 6]. The model includes three important features; (i) duplication, (ii) mutation, and (iii) divergence. (i) At each time step, a node is newly introduced, which duplicates a randomly chosen nodes (called replicated node) among pre-existing nodes. (ii) The node connects to each of the neighbors of the replicated node with probability $1 - \delta$. (iii) The new node also can link to all pre-existing node with probability β/N, where N is the current total number of nodes. Thus cluster merging occurs.

In order to apply the global suppression effect of the r-GRN model to the PIN model, we slightly modify the process (iii) of the PIN models as follows. Each new node links only to the nodes belonging to set $\mathbf{R}$ with the smallest clusters, which is similarly defined in the r-GRN model. The value β in the probability β/gN, where gN is the current total number of nodes belonging to set $\mathbf{R}$, corresponds to p in the r-GRN model. Accordingly, the growth of large clusters is suppressed. From the numerical simulations up to $N = 10^8$ with 1000 ensemble averages, we also observe the abnormal transition behaviors as shown in figure 9, where the previous BKT transition of the PIN model breaks down but the features of infinite-, second-, and first-order type transitions all occur similarly to the r-GRN model.

For $\delta = 0.7$, we numerically simulate for $g = 0.4$ and $g = 0.6$. Figure 10 shows the two transition points $p_b = 0.29(1)$ and $p_c = 0.43(1)$ in panels (a) and (c) for $g = 0.4$, and $p_b = 0.26(1)$ and $p_c = 0.35(1)$ in panels (b) and (d) for $g = 0.6$. The two transition points obtained from the analytical results are consistent with numerical results. This result is also close to that obtained in the r-GRN model. Thus, we argue that our main results are universal independent of detailed model dynamic rules.

J. Stat. Mech. (2019) 083502

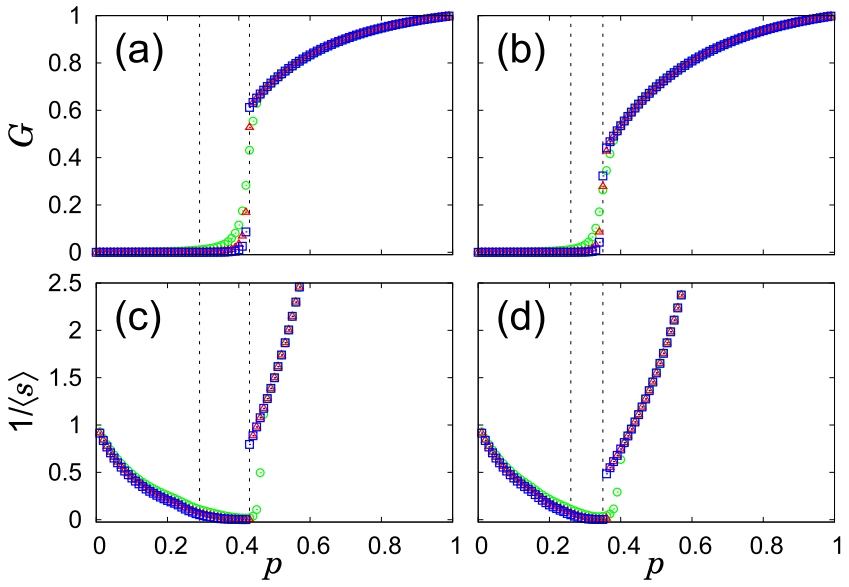

Figure 10. Plot of G and $1/\langle s\rangle$ for the r-PIN model as a function of p for $g = 0.4$ in (a) and (c), and for $g = 0.6$ in (b) and (d), respectively. Symbols represent numerical simulation data for $N = 2^2 \times 10^4$ (green circle), $2^8 \times 10^4$ (red triangle), and $2^{14} \times 10^4$ (blue square). Each data point was averaged over 10^2 configurations. The two vertical dotted lines represent p_b and $p_c > p_b$.

7. Discussion

When the link occupation probability p is below p_c, most clusters are small and the suppression is not effective. Hence the infinite-order critical behavior of $n_s(p) \sim s^{-\tau(p)}$ appears as the one in the Berezinskii–Kosterlitz–Thouless (BKT) transition. The exponent $\tau(p)$ decreases as p is increased. In the BKT transition, τ decreases down to three as p is increased to p_c; however, in this restricted growing random network (r-GRN) model, the exponent $\tau(p)$ can decrease more down to two, because the transition point is delayed by the suppression effect. On the other hand, if the cluster size distribution follows a power law without any exponential cutoff, the largest cluster size scales with the system size $N(t)$ in the steady state as $s_{\max} \sim N^{1/(\tau-1)}$. When τ decreases down to two, the largest cluster grows to the extent of the system size in the steady state. Therefore a discontinuous transition occurs.

As τ decreases below three, the mean cluster size, i.e. the susceptibility is no longer finite. We divide the region $p < p_c$ into two subregions, $p < p_b$ and $p_b < p < p_c$, such that for $p < p_b$, $\tau > 3$, whereas for $p_b < p < p_c$, $2 < \tau < 3$. Thus, the mean cluster size is finite and diverges in the former and latter regions, respectively. Therefore, another type of percolation transition (PT) occurs at p_b. It is interesting to note that the mean cluster size diverges even though the giant cluster does not form yet in the interval $p_b < p < p_c$. That is because the cluster size distribution exhibits a critical behavior without an exponential cutoff. Large clusters still remain in the sub-extensive size, and they induce heavy fluctuations. We regard the region $p < p_b$ as an infinite-order-type critical region, because it is inherited from the infinite-order transition. The region $p_b < p < p_c$, in which the feature of the second-order transition appears, is regarded

J. Stat. Mech. (2019) 083502

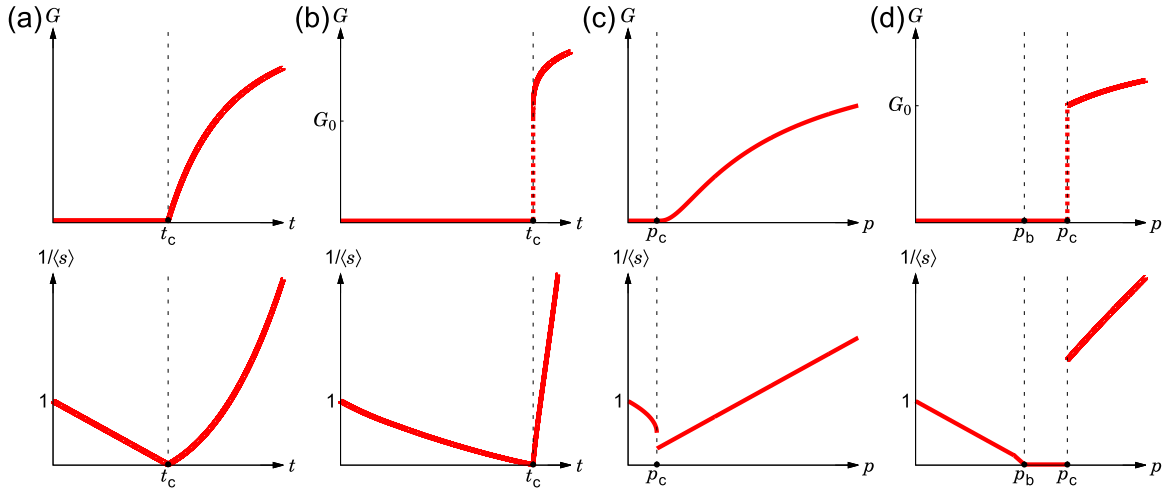

Figure 11. Schematic plots of the order parameter G and the inverse mean cluster size $1/\langle s\rangle$ for the (a) ER, (b) r-ER, (c) GRN, and (d) r-GRN models.

as the second-order-type critical region. At p_c, a first-order PT occurs. For $p > p_c$, the size distribution of finite clusters does not follow a power law. The region $p \geqslant p_c$ is regarded as a supercritical region. Therefore, when the infinite-order BKT transition is broken by the suppression effect, a first-order PT occurs; a second-order critical phase appears; and an infinite-order critical phase still remains. We remark that to the best of our knowledge, this is the first observation of the first-order PT in random growing networks.

The r-GRN model was built based on the restricted Erdős–Rényi (r-ER) model recently introduced in [28, 29]. This r-ER model is a static network model, containing N nodes all the time. The two-node selection rule for a link connection is the same as that of the r-GRN model but once the two nodes are selected at time step t, they are connected definitely. This model contains a global suppression dynamic. In this r-ER model, a power-law behavior of $n_s(t_c)$ without any exponential cutoff appears only at the point t_c^+ just after the order parameter jumps. The exponent τ is in the range $2 < \tau \leqslant 5/2$ depending on the parameter g. Thus, the model exhibits not only a discontinuous transition but also a critical behavior. The critical behavior appears in the region where the order parameter is finite [28]. In contrast to the transition behavior of this r-ER static network model, the critical behavior in the r-GRN model appears below the transition point p_c, so that the order parameter still remains at zero. These behaviors are depicted schematically in figure 11.

For the r-GRN model, the power-law decay of $n_s(p)$ appears in a steady state over all cluster sizes without forming any bump or exponential cutoff even for all $p < p_c$. This reason is as follows: at each time step, a new node is added and remains as isolated with the probability $1 - O(1/N)$, which is close to unity as N becomes large. Thus, single-size nodes are accumulated in the system and they are more likely to merge finite-size clusters, reducing the frequency of merging two large clusters. When dynamics reaches a steady state, the cluster merging dynamics self-organizes and forms a power-law behavior of $n_s(p)$. We considered an extreme case that a new node is merged with an existing cluster at each time step with probability p. In this case, $n_s(p)$ is obtained as $\sim s^{-(1+1/p)}$. More generally, as p is increased, more links are added, and the largest

cluster becomes larger, and thus the exponent $\tau(p)$ is continuously decreasing. Because the transition point is delayed by the suppression effect, τ can decrease down to two. This eventually leads to a discontinuous PT, because the largest cluster size scales as $N(t)^{1/(\tau-1)}$, where $N(t)$ denotes the system size at a certain time t in steady state, and it reaches up to the extensive size to the system size when $\tau = 2$ regardless of t in the steady state.

This tri-critical-like behavior at $\tau = 2$ can be seen in the classical polymer aggregation model [31–35]. The cluster aggregation phenomena in a static system were described via the rate equation,

$$\frac{\mathrm{d}n_s(t)}{\mathrm{d}t} = \sum_{i+j=s} \frac{w_i n_i}{c(t)} \frac{w_j n_j}{c(t)} - 2\frac{w_s n_s}{c(t)} \sum_{i=1} \frac{w_i n_i}{c(t)}, \tag{16}$$

where $c(t) = \sum_s w_s n_s(t)$. The first term on the R.H.S. represents the aggregation of two clusters of sizes i and j with $i + j = s$, and the second term is for a cluster of size s merging with another cluster of any size. The rate equation reduces to the ER network model when $c(t) = 1$, which occurs when $w_i = i$. A general case, $w_i = i^\omega$, was studied [31–35] long ago. In this case, as ω is smaller, the growth of large clusters is more suppressed. When $1/2 < \omega < 1$, a continuous transition occurs at t_c; a giant cluster is generated for $t > t_c$. At $t = t_c$, the cluster size distribution follows a power law with exponent $\tau = \omega + (3/2)$. When $0 < \omega \leqslant 1/2$, a discontinuous transition occurs, and the exponent $\tau = 1 + 2\omega$. The case $\omega = 1/2$, for which $\tau = 2$, is marginal between a second-order and a first-order transition. We remark that another model recent introduced also generates either a continuous or a discontinuous PT by controlling the suppression strength similar to the above case [36]. These two cases are all for static networks. Even though the system type and the underlying mechanism of static and growing networks are different, on the basis of the above result, we could confirm that the discontinuous transition at p_c is induced by the increase of the cluster size heterogeneity across the point with $\tau = 2$.

The BKT transition was found originally in the two-dimensional XY model in thermal systems [8–12]. The origin of the BKT transition in thermal systems is different from that of the percolation model, but some similarities or dissimilarity in the transition behavior exist: in the XY model, the singular part of the free energy behaves as $f(t) \sim \exp(-bt^{-1/2})$ with a positive constant b for the reduced temperature $t = (T - T_c)/T_c > 0$, similar to the order parameter $G(p)$ for $p > p_c$ in equation (1). The correlation function decays in a power-law manner as $\Gamma(r) \sim r^{-\eta(T)}$ for $t < 0$, where $\eta(T) \sim T$ is continuously varying depending on T. This is often called the quasi-long-range order. On the other hand, in a second-order transition $\Gamma(r) \sim r^{-\eta} \exp(-r/\xi)$ for $t < 0$. In this regard, the pure power-law behavior of $\Gamma(r)$ in the infinite-order transition implies $\xi = \infty$ for $t < 0$. Indeed, $\xi = \infty$ for $t < 0$ in the XY model. The continuous varying exponent $\eta(T)$ in the XY model corresponds to the exponent $\tau(p)$ of the cluster size distribution $n_s(p) \sim s^{-\tau(p)}$. In a second-order PT, $n_s \sim s^{-\tau} \exp(-s/s^*)$ for $p < p_c$, where s^* is a characteristic cluster size in the region $p < p_c$. Again, the pure power-law behavior of the infinite-order PT implies that $s^* = \infty$ for $p < p_c$. The susceptibility is obtained using the thermodynamic relation, $\chi \sim \int \mathrm{d}^2 r \Gamma(r)$. One can find that χ diverges for $\eta < 2$, while it is finite for $\eta > 2$. Because η increases with temperature, χ diverges for $t < 0$ and finite for $t > 0$, where the critical temperature is determined by

J. Stat. Mech. (2019) 083502

Table 3. Comparison of the BKT transitions between in thermal systems and in percolations of the growing networks.

Thermal systems	Percolation
$f(t) \sim \exp(-bt^{-1/2})$, $t = (T - T_c)/T_c$	$G(p) \sim \exp(-a(p - p_c)^{-1/2})$
$\chi \sim \int \mathrm{d}^2 r \Gamma(r) \sim \int \mathrm{d}r r \Gamma(r)$	$\chi = \sum s^2 n_s \approx \int \mathrm{d}s s p(s)$
$\Gamma(r) \sim r^{-\eta(T)}$ for $t < 0$	$p(s) = s n_s \sim s^{1-\tau}$ for $p < p_c$
$\eta(T) \sim T < 2$ for $\chi = \infty$	$\tau = \tau(p) < 3$ for $\chi = \infty$
$\xi = \infty$ for $t < 0$	$s^*(p) = \infty$ for $p < p_c$
$\tau(p) > 3$ for $p < p_c$ in the original growing percolation	
$\tau(p) > 2$ for $p < p_c$ in the restricted growing percolation	

$\eta = 2$. In percolation, the susceptibility $\chi = \sum_s s^2 n_s$ diverges for $\tau < 3$, while it is finite for $\tau > 3$. For the GRN model, $\tau > 3$ for $p < p_c$. Thus, the susceptibility is finite for $p < p_c$. For $p > p_c$, n_s of finite clusters decays exponentially. Thus the susceptibilities on both sides of a transition point are finite. Even though the order parameter behaves as an infinite-order transition, the susceptibility behavior is different from that of the XY model. On the other hand, for the r-GRN model, the susceptibility diverges in one side and is finite in the other side, similar to those of the XY model. These properties are all summarized in table 3.

The BKT transition can occur even in static networks. For instance, the percolation model in one dimension with $1/r^2$ long-range connections [22] and on hierarchical networks with short-range and long-range connections [37] exhibit BKT infinite-order PTs. As future works, it would be interesting to check whether the diverse phases and phase transitions we obtained occur or not in those static network models when the suppression rule is applied. Moreover, in our study, the suppression rule is applied to large clusters, because the giant cluster size per node is the order parameter in percolation problem. As an extension of our work to thermal systems, it would be interesting to find an essential quantity of thermal BKT systems, for instance, the formation of spin waves or vortices, and see if we can control the BKT transition by the suppression effect. The pattern formation by topological defects in active liquid crystals recently draws considerable attention [38, 39]. Various patterns generated in that system are governed basically by the BKT theory. It would be interesting to note how those patterns are changed when the system is applied by a certain suppression effect.

8. Summary

In summary, we investigated how a BKT PT of growing networks is changed in type when the growth of large clusters in the system is suppressed. We introduced the r-GRN model, modified from the GRN model by including the suppression rule. In the r-GRN model, we found that two transition points exist, p_b and p_c, and three phases. (i) In the region $p < p_b$, the order parameter is zero, and the cluster size distribution decays according to a power law without any exponential cutoff and with exponent

J. Stat. Mech. (2019) 083502

$\tau(p)$ larger than three. Thus, the mean cluster size is finite. The exponent $\tau(p)$ continuously decreases as p is increased. Accordingly, the region $p < p_b$ is regarded as an infinite-order type critical region. (ii) For the $p_b < p < p_c$ region, we found that the order parameter is zero, and the cluster size distribution follows a power law without any exponential cutoff, where the exponent $\tau(p)$ ranges between two and three. Thus, the mean cluster size diverges. This behavior is reminiscent of the critical behavior occurring at the critical point of a second-order transition. Thus, region (ii) is regarded as a second-order type critical region. The fact that the mean cluster size diverges, even though the largest cluster has not grown to the extensive size yet, implies that the fluctuations of sub-extensive-finite clusters diverge preceding to the emergence of the giant cluster of extensive size. Similar behavior occurs in a hierarchical model [40]. (iii) At p_c, a discontinuous transition occurs. (iv) The region $p > p_c$ is regarded as a noncritical region because the order parameter is finite, and the cluster size distribution decays exponentially. Thus, our model contains the three regimes of the infinite-order, second-order, and first-order transitions. We obtained various properties of the transition behaviors analytically and numerically. We also found that PIN models exhibit the BKT transitions and obtain a similar pattern of PT to those in the r-GRN model. Thus our main results are universal, independent of detailed dynamic rules.

Acknowledgment

This research was supported by the National Research Foundation of Korea (NRF) through Grant No. NRF-2014R1A3A2069005 (BK) and No. NRF-2017R1D1A1B03032864 (SWS), and a TJ Park Science Fellowship from the POSCO TJ Park Foundation (SWS).

Appendix. Rate equations of the r-GRN model

Here we recall the rate equations previously derived in [25]. The cluster number density $n_s(p,t)$ is defined as the number of clusters of size s divided by $N(t)$ at time step t, where p denotes the probability that a link is connected between two selected nodes. We denote the size of the largest cluster in set $\mathbf{R}$ as $S_R(p,t)$. Then the rate equations of $n_s(p,t)$ are as follows:

$$\frac{\mathrm{d}(N(t)n_s)}{\mathrm{d}t} = p\Big[\sum_{i,j=1}^{\infty}\frac{in_i jn_j}{g}\delta_{i+j,s} - sn_s - \frac{sn_s}{g}\Big] + \delta_{1s}\text{for}\quad s < S_R, \tag{A.1}$$

$$\frac{\mathrm{d}(N(t)n_s)}{\mathrm{d}t} = p\Big[\sum_{i,j=1}^{\infty}\frac{in_i jn_j}{g}\delta_{i+j,s} - sn_s - \Big(1 - \sum_{k=1}^{S_R-1}\frac{kn_k}{g}\Big)\Big] + \delta_{1s}\text{for}\quad s = S_R, \tag{A.2}$$

$$\frac{\mathrm{d}(N(t)n_s)}{\mathrm{d}t} = p\Big[\sum_{j=1}^{\infty}\sum_{i=1}^{S_R-1}\frac{in_i jn_j}{g}\delta_{i+j,s} + \sum_{j=1}^{\infty}\delta_{S_R+j,s}jn_j\Big(1 - \sum_{k=1}^{S_R-1}\frac{kn_k}{g}\Big) - sn_s\Big]\text{for}\quad s > S_R. \tag{A.3}$$

On the R.H.S. of equation (A.1) for $s < S_R$, the first gain term $\sum_{i,j=1}^{\infty}\frac{in_i jn_j}{g}\delta_{i+j,s}$ means the probability that one node is randomly selected in set $\mathbf{R}$ and the other is randomly

J. Stat. Mech. (2019) 083502

selected from the entire system, and they are merged and then generate a cluster of size s. The second and third terms $(1+1/g)sn_s$ means the probability that one node is randomly selected from a cluster of size s in set $\mathbf{R}$ regardless of the other node selected from all other nodes in the entire system and vice versa. The last term, δ_{1s} represents the contribution by an incoming isolated node at each time step. In equation (A.2) for $s = S_R$, the first, second, and the last terms are obtained in the same way as in equation (A.1). The third term $1-\sum_{k=1}^{S_R-1}\frac{kn_k}{g}$ means the probability that one node is randomly selected from the largest cluster of size S_R in set $\mathbf{R}$ regardless of the other node selected from all nodes in the entire system. In equation (A.3) for $s > S_R$, the first term $\sum_{j=1}^{\infty}\delta_{i+j,s}jn_j\sum_{i=1}^{S_R-1}\frac{in_i}{g}$ means the probability that one node is randomly selected from the nodes, which do not belong to the cluster of size S_R in set $\mathbf{R}$ and the other node randomly selected in all nodes that generates a cluster of size $s > S_R$. The second term $\sum_{j=1}^{\infty}\delta_{S_R+j,s}jn_j\left(1-\sum_{i=1}^{S_R-1}\frac{in_i}{g}\right)$ means the probability that one node is randomly selected from the cluster of size S_R in set R and the other node randomly selected from all nodes in the entire system. The third loss term sn_s is obtained in the same way as in equation (A.1) and (A.2). p means the probability that two selected nodes are linked.

In the steady state $t\to\infty$, $S_R(p,t)$ and $n_s(p,t)$ become independent of t, and they are written as $S_R(p)$ and $n_s(p)$, respectively. Then the L.H.S. of equations (A.1)–(A.3) become $n_s(p)$ and the R.H.S. of equations (A.1)–(A.3) are rewritten as follows:

$$n_s = p\Big[\sum_{i,j=1}^{\infty}\frac{in_ijn_j}{g}\delta_{i+j,s}-\Big(1+\frac{1}{g}\Big)sn_s\Big]+\delta_{1s}\text{for}\quad s<S_R, \tag{A.4}$$

$$n_s = p\Big[\sum_{i,j=1}^{\infty}\frac{in_ijn_j}{g}\delta_{i+j,s}-sn_s-\Big(1-\sum_{k=1}^{S_R-1}\frac{kn_k}{g}\Big)\Big]+\delta_{1s}\text{for}\quad s=S_R, \tag{A.5}$$

$$n_s = p\Big[\sum_{j=1}^{\infty}\sum_{i=1}^{S_R-1}\frac{in_ijn_j}{g}\delta_{i+j,s}+\sum_{j=1}^{\infty}\delta_{S_R+j,s}jn_j\Big(1-\sum_{k=1}^{S_R-1}\frac{kn_k}{g}\Big)-sn_s\Big]\text{for}\quad s>S_R. \tag{A.6}$$

References

[1] Newman M E 2004 Coauthorship networks and patterns of scientific collaboration *Proc. Natl Acad. Sci. USA* **101** 5200

[2] Lee D, Goh K-I, Kahng B and Kim D 2010 Complete trails of coauthorship network evolution *Phys. Rev.* E **82** 026112

[3] Leskovec J, Kleinberg J and Faloutsos C 2007 Graph evolution: densification and shrinking diameters *ACM Trans. Knowl. Discov. Data* **1** 2

[4] Solé R V, Pastor-Satorras R, Smith E D and Kepler T 2002 A model of large-scale proteome evolution *Adv. Complex Syst.* **05** 43

[5] Vázquez A, Flammini A, Maritan A and Vespignani A 2003 Modeling of protein interaction networks *ComPlexUs* **1** 38

[6] Kim J, Krapivsky P L, Kahng B and Redner S 2002 Infinite-order percolation and giant fluctuations in a protein interaction network *Phys. Rev.* E **66** 055101

[7] Callaway D S, Hopcroft J E, Kleinberg J M, Newman M E J and Strogatz S H 2001 Are randomly grown graphs really random? *Phys. Rev.* E **64** 041902

J. Stat. Mech. (2019) 083502

[8] Berezinskii V L 1971 Destruction of long-range order in one-dimensional and two-dimensional systems having a continuous symmetry group I. Classical systems *Sov. Phys.—JETP* **32** 493
[9] Berezinskii V L 1972 Destruction of long-range order in one-dimensional and two-dimensional systems possessing a continuous symmetry group II. Quantum systems *Sov. Phys.–JETP* **34** 601
[10] Kosterlitz J M and Thouless D J 1972 Long range order and metastability in two dimensional solids and superfluids *J. Phys. C: Solid State Phys.* **5** L124
[11] Kosterlitz J M and Thouless D J 1973 Ordering, metastability and phase transitions in two-dimensional systems *J. Phys. C: Solid State Phys.* **6** 1181
[12] Kosterlitz J M 1974 The critical properties of the two-dimensional XY model *J. Phys. C: Solid State Phys.* **7** 1046
[13] Kosterlitz J M 2017 Nobel lecture: topological defects and phase transitions *Rev. Mod. Phys.* **89** 040501
[14] Haldane F D M 2017 Nobel lecture: topological quantum matter *Rev. Mod. Phys.* **89** 040502
[15] Dorogovtsev S N, Mendes J F F and Samukhin A N 2001 Anomalous percolation properties of growing networks *Phys. Rev.* E **64** 066110
[16] Jaeger G 1998 The Ehrenfest classification of phase transitions: introduction and evolution *Arch. Hist. Exact. Sci.* **53** 51–81
[17] Oh S M, Son S-W and Kahng B 2016 Explosive percolation transitions in growing networks *Phys. Rev.* E **93** 032316
[18] Yi S D, Jo W S, Kim B J and Son S-W 2013 Percolation properties of growing networks under an achlioptas process *Europhys. Lett.* **103** 26004
[19] Jo W S, Kim B J, Yi S D and Son S-W 2014 Structural properties of networks grown via an achlioptas process *J. Korean Phys. Soc.* **65** 1985
[20] Stauffer D and Aharony A 1994 *Introduction to Percolation Theory* (London: Taylor and Francis)
[21] Cohen R, Erez K, ben-Avraham D and Havlin S 2000 Resilience of the internet to random breakdowns *Phys. Rev. Lett.* **85** 4626
[22] Grassberger P 2013 SIR epidemics with long-range infection in one dimension *J. Stat. Mech.* P04004
[23] Riordan O and Warnke L 2011 Explosive percolation is continuous *Science* **333** 322
[24] Cho Y S, Hwang S, Herrmann H J and Kahng B 2013 Avoiding a spanning cluster in percolation models *Science* **339** 1185
[25] Oh S M, Son S-W and Kahng B 2018 Suppression effects on the Berezinskii–Kosterlitz–Thouless transitions in growing networks *Phys. Rev.* E **98** 060301
[26] Erdős P and Rényi A 1960 On the evolution of random graphs *Publ. Math. Inst. Hung. Acad. Sci.* A **5** 17
[27] Panagiotou K, Sphöel R, Steger A and Thomas H 2011 Explosive percolation in Erdős-Rényi-like random graph processes *Electron. Notes Discrete Math.* **38** 699
[28] Cho Y S, Lee J S, Herrmann H J and Kahng B 2016 Hybrid percolation transition in cluster merging processes: continuously varying exponents *Phys. Rev. Lett.* **116** 025701
[29] Choi K, Lee D, Cho Y S, Thiele J C, Herrmann H J and Kahng B 2017 Critical phenomena of a hybrid phase transition in cluster merging dynamics *Phys. Rev.* E **96** 042148
[30] Solé R V and Pastor-Satorras R 2002 Complex networks in genomics and proteomics *Handbook of Graphs and Networks* ed S Bornholdt and H G Schuster (Berlin: Wiley)
[31] Ziff R M, Hendriks E M and Ernst M H 1982 Critical properties for gelation: a kinetic approach *Phys. Rev. Lett.* **49** 593
[32] Levyraz F and Tschudi H R 1981 Singularities in the kinetics of coagulation processes *J. Phys. A: Math. Gen.* **14** 3389
[33] Cho Y S, Kahng B and Kim D 2010 Cluster aggregation model for discontinuous percolation transitions *Phys. Rev.* E **81** 030103
[34] Son S-W, Bizhani G, Christensen C, Grassberger P and Paczuski M 2011 Irreversible aggregation and network renormalization *Europhys. Lett.* **95** 58007
[35] Son S-W, Christensen C, Bizhani G, Grassberger P and Paczuski M 2011 Exact solutions for mass-dependent irreversible aggregations *Phys. Rev.* E **84** 040102
[36] Bianconi G 2018 Rare events and discontinuous percolation transitions *Phys. Rev.* E **97** 022314
[37] Berker A N, Hinczewski M and Netz R R 2009 Critical percolation phase and thermal Berezinskii–Kosterlitz–Thouless transition in a scale-free network with short-range and long-range random bonds *Phys. Rev.* E **80** 041118
[38] Marchetti M C, Joanny J F, Ramaswamy S, Liverpool T B, Prost J, Rao M and Aditi Simha R 2013 Hydrodynamics of soft active matter *Rev. Mod. Phys.* **85** 1143
[39] Tang X and Selinger J 2017 Orientation of topological defects in 2D nematic liquid crystals *Soft. Matter* **13** 5481
[40] Boettcher S, Singh V and Ziff M R 2012 Ordinary percolation with discontinuous transitions *Nat. Commun.* **3** 787

J. Stat. Mech. (2019) 083502